Spectroscopy of hydrogenlike and heliumlike argon

J. P. Briand, J. P. Mossé, P. Indelicato, P. Chevallier, D. Girard-Vernhet, and A. Chetioui
Section de Physique et Chimie et Université Pierre et Marie Curie, Institut Curie, 11 rue Pierre et Marie Curie, F-75231 Paris Cédex 05, France*

M. T. Ramos
Laboratorio de Fisica da Universidade de Lisboa, Universidade de Lisboa, Lisboa, Portugal

J. P. Desclaux
Départment de Recherche Fondamentale, Laboratoire d'Interactions Hyperfines, Centre d'Etudes Nucléaires de Grenoble, Boîte Postale 85X, F-38041 Grenoble Cédex, France
(Received 12 November 1982)

The x-ray transitions ($n=2 \rightarrow n=1$) emitted by fast hydrogenlike and heliumlike argon ions have been studied. The absolute energy of the Lyman α lines of hydrogenlike ions has been measured and the value of the ($1s$) Lamb shift of argon evaluated for the first time. The $^3P_{1,2}$ and $^1P_1$ transitions of heliumlike argon have also been studied at very high precision and their energies compared to multiconfiguration Dirac-Fock calculations. The energies of Lyman α lines are of 3323.2 ± 0.5 eV (Lyα_1) and 3318.1 ± 0.5 eV (Lyα_2), and those of $n=2 \rightarrow n=1$ transitions for heliumlike argon are of 3123.6 ± 0.25 eV ($^3P_1$), 3126.4 ± 0.4 eV ($^3P_2$), and 3139.6 ± 0.25 eV ($^1P_1$).

I. INTRODUCTION

In the past, the one- and two-electron heavy ions have mainly been produced and studied in solar corona or fusion plasmas where their characteristic emission lines are used for temperature and density diagnostics. They also constitute, in atomic physics, the most elementary systems for studying the relativistic corrections and the quantum electrodynamic effects in the electron-electron interaction in bound states. These effects are of great importance in heavy atoms and cannot be specifically studied in many-electron systems. These ions can now be studied, either in gas targets irradiated by high-velocity heavy ions or in flight. The former created atomic ions in which the electrons are removed in a single event (recoil ions). The latter generated ions by passing through thin carbon foils. These high-velocity ion beams are delivered by the most powerful accelerators of nuclear physics. In this paper, we describe experiments in which the hydrogenlike and heliumlike argon ions have been studied with high-resolution x-ray spectroscopy. These ions were produced by the heavy-ion cyclotron of the Institut de Physique Nucléaire in Orsay (CEVIL). The x-ray spectra emitted by these hydrogenlike and heliumlike ions, when excited through thin carbon foils to the $n=2$ state (directly or following cascades), have been observed with a plane crystal spectrometer and absolute energies of the lines determined by direct comparison with well-known characteristic x rays.

TABLE I. Measured equilibrium state distribution for 240-MeV argon ions (Ref. 1) after 100-μg-cm^{-2} carbon foil.

Ar^{18+} (bare nucleus)	Ar^{17+} (hydrogenlike)	Ar^{16+} (heliumlike)
20%	42%	29%

II. EXPERIMENTAL

The equilibrium charge state distribution, which was obtained after stripping the 240-MeV Ar^{12+} beam in 100-μg-cm^{-2} carbon foil, is presented in Table I. After being stripped, the beam was excited in a second, very thin carbon foil in some of the experiments. The main excitation process in this experimental situation was the capture of a target electron in an excited state of bare ions (producing hydrogenlike ions) or one-electron ions (producing heliumlike singly excited ions). The radiative decay of all these species mostly takes place in a very short range after the foil (< 10 μm). When carbon foils were put perpendicular to the beam, the beam acted like a linear x-ray source of negligible thickness. In order to improve the resolution of the spectrometer, downgraded by Doppler broadening, the angular divergence of the beam was limited to 1 milliradian. To get a 1-cm spot in the horizontal plane, the beam intensity had to be reduced by a factor of 6 on the target

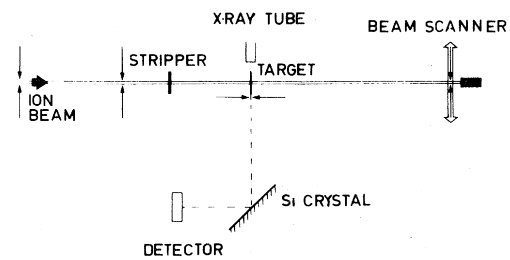

FIG. 1. Schematics of the experimental setup.

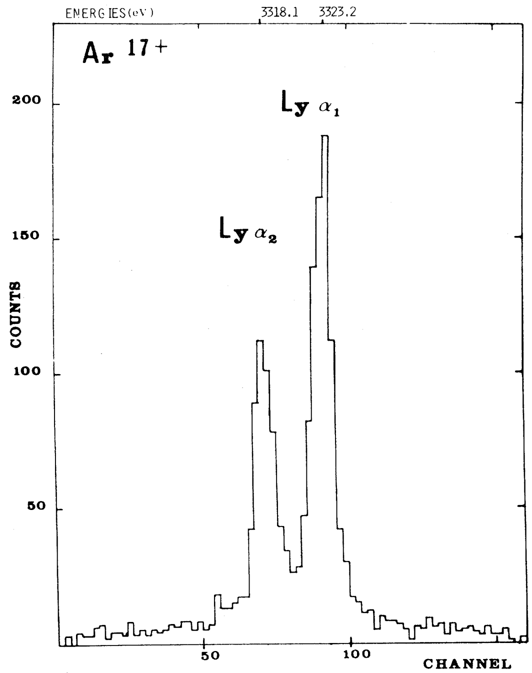

FIG. 2. Lyman α spectrum of hydrogenlike argon ions.

(conservation of the emittance of the beam). The direction and homogeneity of the beam were determined by moving a small slit in front of the Faraday cup downstream from the target. The mean direction of the ions was defined within a precision of 10^{-2} deg and the homogeneity of the beam was known within $\pm 5\%$.

The design of the spectrometer is presented in Fig. 1 (Ref. 2). The entrance slit, located as close as possible to the target, was made of two thorium lips parallel to the ion beam. One of the lips was fixed and the other accurately controlled by a 1-μm stepping motor. The width of the slit was usually of the order of 150 μm. After passing through the slit, the x rays were reflected by a Si(111) plane crystal, located 1.5 m away from the target. The crystal was mounted under vacuum, on a precision goniometer (3×10^{-4} deg) controlled by a stepping motor. The reflected x rays were detected in a position-sensitive detector of the Backgammon type. Owing to the very strong absorption of x rays of $\sim$3 keV in air, the detector was mounted close to the beryllium foil which sealed the vacuum chamber of the spectrometer. The position-sensitive detector was moved along a circular track around the axis of the goniometer. Its position was known with a high precision (a few μm) compared to the spatial resolution (100 μm) of the detector. The principle of the energy measurements was to accurately determine the difference of the Bragg angles between the lines under study and some well-known reference lines. The absolute energy of the Lyman α lines of hydrogenlike argon was determined with respect to that of potassium $K\alpha$ lines emitted by a KCl anode irradiated by a 9-keV electron beam. The energy of the heliumlike lines was determined with respect to that of the hydrogenlike Lyman α lines. The second carbon target was mounted on a special holder such that the x rays emitted at the surface of the foil could be detected without any absorption. The holder was mounted on a goniometer and a translator in order to adjust the position of the x-ray source with respect to the slit.

TABLE II. Top: theoretical and experimental energy values (in eV) of Lyman α lines of hydrogenlike argon. [Potassium $K\alpha$ line energies in KCl used in the measurement are those given in Bearden's table (Ref. 4).] Bottom: Comparison between experimental and theoretical values (in eV) of the (1s) Lamb shift of hydrogenlike argon.

Transition	Expt. (eV)	Theory (eV)	Expt.-Theor. (eV)
Lyman α_1	3323.2±0.5	3323.05	+0.15
Lyman α_2	3318.1±0.5	3318.23	−0.13
1s Lamb shift	1.0±0.5	1.135	

III. THE HYDROGENLIKE SPECTRA

In Fig. 2, we present the Lyman α lines of hydrogenlike argon. The precision of the absolute energy values of the considered lines depends on various parameters. The first of these are the geometric parameters of the ion beam with respect to those of the detected x rays (Doppler effect). As was previously described, the direction of the ions with respect to the mechanical axis of the beam pipe was defined with a precision of 10^{-2} deg (0.07 eV). The line of flight of the detected x rays was established as normal to

TABLE III. Various contributions to the energy of the levels in hydrogenlike argon. Fundamental constants and the nuclear data are those given in Refs. 5 and 6. Total (1s) Lamb shift (+1.135 eV) and the total $2p_{1/2}$ Lamb shift (−0.015 eV) are those given by P. Mohr (Ref. 7) and deduced from Wichmann and Kroll (vacuum polarization) (Ref. 8).

Contribution	$1s_{1/2}$	$2p_{1/2}$	$2p_{3/2}$
Dirac	−4427.521	−1108.081	−1103.276
Nuclear mass	+0.061	+0.015	+0.015
Nuclear volume	+0.018	+0.002	+0.002
QED			
Self-energy	+1.221	−0.004	+0.006
Vacuum polarization	−0.086	−0.0107	
Total	−4426.307	−1108.079	−1103.253

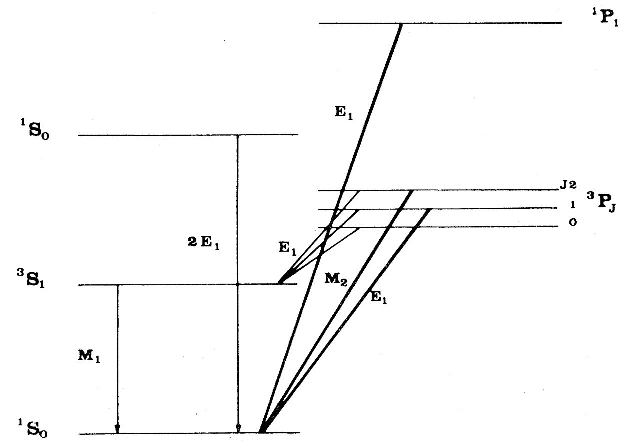

FIG. 3. Decay scheme of heliumlike ions.

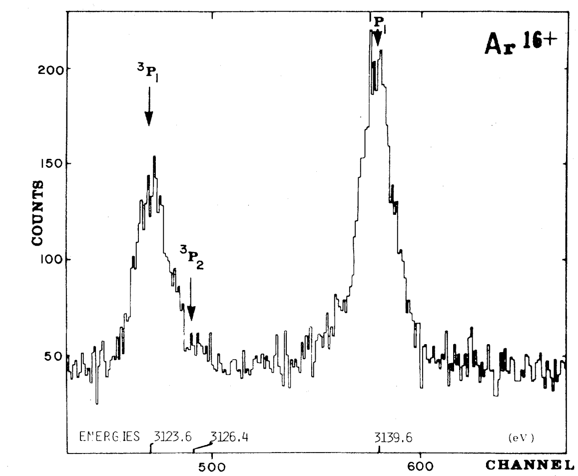

FIG. 4. $(1s)(2p) \rightarrow (1s)^2$ spectrum of heliumlike argon.

the velocity of the ions by reflecting a laser beam through a semireflective, right-angle prism whose right angle was known with an accuracy of 2×10^{-3} deg. The laser beam was then reflected back on itself by aligning the cut face of the crystal parallel to the beam. The overall accuracy of this measurement was of the order of 10^{-2} deg (0.07 eV), introducing an error of 0.15 eV in the Doppler correction of the measured energy. The energy of the beam was accurately known with a relative precision of 4×10^{-3}, either by measuring the deflection angle of the particles in an accurately known magnetic field or by proton recoil (Ref. 3). This introduces an overall error of 0.15 eV in the x-ray measurement.

Two important sources of error in the measurement are caused by the energy calibration of the spectrometer and the statistical error in the determination of the centroid of the considered peaks. These errors were estimated to be 0.15 eV, leading to an overall uncertainty of <0.5 eV.

In Table II, we present the experimental values of the Lyman α_1 and Lyman α_2 lines obtained after averaging some independent measurements. These energies have to be compared with theoretical ones (Table III). The theoretical energies are those given by the difference of the Dirac eigenvalue, corrected for the nuclear-size effects, minus the $1s$ Lamb shift. (The $2p$ Lamb shift has been ignored because it is less than 10^{-2} eV.) All the contributions to the $1s$ Lamb shift—self-energy and vacuum polarization—are presented in Table III. The agreement between the theory and the experiment is found to be better than 0.15 eV. The $1s$ Lamb shift is found to be 1.0 ± 0.5 eV, while the total theoretical radiative correction is 1.135 eV. It should be pointed out that this absolute energy measurement constitutes the first comparison between an x-ray line and an exact theoretical prediction for a one-electron ion.

IV. THE HELIUMLIKE SPECTRA

Of the four possible lines in the decay of the $n=2$ levels to the ground state (Fig. 3), only three can be detected near the foil, the $M1$ forbidden transition having too long a lifetime to be detected through a 150-μm slit. In Fig. 4, we present one of the observed heliumlike spectra, and in Table IV the experimental energy values. These energies have been deduced from the theoretical values of the Lyman α line, leading to a great improvement in the precision of the energy, ±0.25 eV. (The error only comes from the statistical uncertainty in the determination of the centroid of the peaks and the uncertainty in the measurements of the angle.) These energies are compared to previous measurements in Table IV. We must, however, be careful when comparing these data, even if they seem to agree fairly well, because of the different conditions in which these values were obtained. The main problem in measuring the absolute energy of a line is to be free from satellite lines, it means not having any excited spectator electrons in the ion. The presence of an excited spectator electron can "in principle" be detected in the x-ray spec-

TABLE IV. Comparison of our energy values (in eV) and previous measurements for the $n=2\rightarrow n=1$ transitions in heliumlike argon.

Transition	This work	Neupert Reference 9	Dohmann and Mann Reference 10
$(1s)^2\,{}^1S_0$-$(1s)(2p)\,{}^1P_1$	3139.6 ± 0.25	3138.9 ± 0.9	3140.1 ± 0.7
$(1s)^2\,{}^1S_0$-$(1s)(2p)\,{}^3P_1$	3123.6 ± 0.25	3123.8 ± 0.9	
$(1s)^2\,{}^1S_0$-$(1s)(2p)\,{}^3P_2$	3126.4 ± 0.4		3126.6 ± 0.7

TABLE V. Comparison of our experimental energy values and theoretical energy values for $n=2\rightarrow n=1$ heliumlike transitions in argon.

Transition	Experiment	Desclaux (this work)	Safronova Reference 12	Drake Reference 13[a]	Johnson Reference 14[a]	Grabriel Reference 15
$(1s)^2\,{}^1S_0$-$(1s)(2p)\,{}^1P_1$	3139.6±0.25	3139.7	3139.56	3139.69	3140.15	3140.46
$(1s)^2\,{}^1S_0$-$(1s)(2p)\,{}^3P_1$	3123.6±0.25	3123.6	3123.59	3123.63	3123.47	3123.84
$(1s)^2\,{}^1S_0$-$(1s)(2p)\,{}^3P_2$	3126.4±0.4	3126.3	3126.32		3126.15	3126.99

[a]Energy corrected for QED using values quoted in Table VI.

tra. If the extra electron is in the $n=2$ shell, the lines are very strongly shifted in energy with respect to those of the "pure" heliumlike ion (diagram lines) and easily detected. If the extra electron is captured in an $n>2$ shell, the energy shifts are very small and usually of the same order of magnitude as the observed linewidths. This leads to a contamination of the lines which moves the center of gravity of the observed lines. The branching ratio for electron capture in various shells of the ion depends on the exact nature of the process, but is usually constant. The presence in the spectrum of far satellites indicates the contamination of the observed "diagram" lines.

In the Neupert experiment (Ref. 9) the heliumlike argon ions were observed in the solar corona plasma, i.e., a situation in which the dielectronic recombination plays a dominant role. We can then expect significant energy shift of the x rays.

In the Dohmann experiment (Ref. 10), the ions were produced in a beam-foil experiment, as in this experiment, but at a much lower energy, i.e., a situation in which electron-capture processes in $n=2,3,4$ shells are very likely. This then produced an intense lithiumlike spectrum which indicated the presence of "contamination satellites."

In the present experiment, the electron-capture process was very unlikely because of the large energy of the ions. This strongly reduces the counting rate as well as the satellite formation. In the observed spectrum, we did not observe any far satellite lines (lithiumlike), indicating that we were observing pure diagram lines. A more detailed discussion of these effects will be presented elsewhere (Ref. 11).

Until now, there have been many calculations of the energy levels of the heliumlike argon ion but no precise absolute energy measurements. The results of these calculations (Z expansion, random-phase approximation, and "unified theory") are presented in Table V. To match the high precision in our energy measurement, we have performed multiconfiguration Dirac-Fock calculations which are also presented in Table V. These calculations are compared to the experimental results, and a good agreement between both, within 0.1 eV, is found which needs to be discussed in more detail. With such precision, all the usually small corrections in the theoretical calculations have to be taken carefully into consideration. In Table VI, various contributions to the energy of the lines are presented. Among the important effects presented in the calculations, one must note the following: the screening of the QED effects—the values we considered for heliumlike ions were appreciably smaller than those for hydrogenlike ions, 0.99 eV instead of 1.135 eV; the correlation energy—which required a large number of additional configurations (see also Table VII) to estimate; and the Breit interaction—which has different values for different lines ($1s2p$ states).

Another point which must be accounted for in the calculations is the influence of extra configurations on the Breit term. We have performed calculations of this effect ("magnetic correlation effects") and presented the results in Table VII. It is apparent that these relativistic correlation effects begin to play a nonnegligible role in this ion of quite large atomic number. These effects, which will play a more important role in ions of higher Z, are also described in more detail in Ref. 14 along with the method of calculation.

ACKNOWLEDGMENTS

Many people have made this work possible. We would like to thank the staff of the heavy-ion cyclotron of the Institut de Physique Nucléaire in Orsay (CEVIL) for their work on the ion beam, and the technical staff of the Laboratoire Curie. We also thank Dr. M. Tavernier for his help during the experiment.

TABLE VI. Contribution of various terms in the energy of the $n=2\rightarrow n=1$ transitions in heliumlike argon (in eV) obtained by multiconfigurational Dirac-Fock calculations.

Contribution	$(1s)^2\,{}^1S_0$-$(1s)(2p)\,{}^1P_1$	$(1s)^2\,{}^1S_0$-$(1s)(2p)\,{}^3P_1$	$(1s)^2\,{}^1S_0$-$(1s)(2p)\,{}^3P_2$
Hartree-Fock	3126.39	3111.78	3111.78
Dirac corr.	15.19	13.43	16.35
Breit interact.	−2.04	−1.79	−1.97
QED	−0.99	−1.02	−1.01
Correlation	1.18	1.18	1.17
Total	3139.73	3123.58	3126.32

TABLE VII. Contributions of various configurations to the correlation energy and Breit term (in eV) for Ar^{16+} $^1S_0$. Numbers of parentheses are powers of ten.

Configuration	Total E[a]	ΔE[b]	Breit term	Weights[c]
$1s^2$	8549.872	0	−2.013	0.999 207
$+ 2s^2$	8550.244	0.372	−1.988	0.281 7(−4)
$+ 3s^2$	8550.270	0.398	−1.984	0.573 4(−6)
$+ 2p^2$	8550.897	1.025	−1.928	0.468 3(−4)
$+ 3p^2$	8550.959	1.087	−1.918	0.148 1(−5)
$+ 3d^2$	8551.036	1.164	−1.909	0.230 0(−5)

[a]Without Breit and QED corrections.
[b]Contribution of the Coulombic correlation energy.
[c]Weights of the configuration.

*Equipe associée au CNRS No. 1018.

[1]Baron, Thèse d'Etat, Université d'Orsay, 1975 (unpublished).

[2]J. P. Briand, M. Tavernier, P. Indelicato, R. Marrus, and H. Gould, Phys. Rev. Lett. 50, 832 (1983).

[3]R. Bimbot, C. Cabot, J. Depauw, D. Gardes, H. Gauvin, L. Martial, A. Richaume, and M. F. Rivet, Institut de Physique Nucléaire d'Orsay Report No. RC 79-03, 1976 (unpublished).

[4]J. A. Bearden, Rev. Mod. Phys. 39, 78 (1967).

[5]E. R. Cohen and B. N. Taylor, J. Phys. Chem. Ref. Data 2, 663 (1973).

[6]G. W. Erickson, J. Phys. Chem. Ref. Data 6, 831 (1977).

[7]P. Mohr, Ann. Phys. (N.Y.) 88, 26 (1974); Phys. Rev. Lett. 34, 1050 (1975); Phys. Rev. A 26, 2338 (1982).

[8]E. H. Wichmann and N. M. Kroll, Phys. Rev. 101, 843 (1956).

[9]W. N. Neupert, Solar Phys. 18, 474 (1971).

[10]H. D. Dohmann and R. Mann, Z. Phys. A 291, 15 (1979).

[11]J. P. Briand, M. Tavernier, R. Marrus, H. Gould, and J. P. Desclaux (unpublished).

[12]U. I. Safronova, Phys. Scr. 23, 241 (1981).

[13]G. W. F. Drake, Phys. Rev. A 19, 1387 (1979).

[14]W. R. Johnson and C. D. Lin, Phys. Rev. A 14, 565 (1976).

[15]A. H. Gabriel, Mon. Not. R. Astron. Soc. 160, 99 (1972).